
PRINCIPAL CONTEXT-AWARE DIFFUSION GUIDED DATA AUGMENTATION FOR FAULT LOCALIZATION

ShihaoFu

School of Big Data and Software Engineering
Chongqing University
Chongqing
fushihao@cqu.edu.cn

YanLei

School of Big Data and Software Engineering
Chongqing University
Chongqing

ABSTRACT

Test cases are indispensable for conducting effective fault localization (FL). However, test cases in practice are severely class imbalanced, *i.e.* the number of failing test cases (*i.e.* minority class) is much less than that of passing ones (*i.e.* majority class). The severe class imbalance between failing and passing test cases have hindered the FL effectiveness.

To address this issue, we propose PCD-DAug : a Principal Context-aware Diffusion guided Data Augmentation approach that generate synthesized failing test cases for improving FL. PCD-DAug first combines program slicing with principal component analysis to construct a principal context that shows how a set of statements influences the faulty output via statistical program dependencies. Then, PCD-DAug devises a conditional diffusion model to learn from principle contexts for generating synthesized failing test cases and acquiring a class balanced dataset for FL. We conducted large-scale experiments on six state-of-the-art FL approaches and compare PCD-DAug with six data augmentation baselines. The results show that PCD-DAug significantly improves FL effectiveness, *e.g.* achieving average improvements of 383.83%, 227.08%, and 224.19% in six FL approaches under the metrics Top-1, Top-3, and Top-5, respectively.

Keywords fault localization, class imbalance, program dependencies, diffusion model.

1 Introduction

With the rapid development of large-scale software systems, effective fault localization (FL) methods have become crucial. Over the years, numerous FL approaches (*e.g.* [1, 2, 3, 4, 5, 6, 7, 8, 9, 10, 11, 12, 13]) have been proposed to identify faulty statements in programs. These approaches typically fall into two categories: spectrum-based fault localization (SFL) [5, 14] and deep learning-based fault localization (DLFL) [9, 15, 16]. Both approaches rely on the execution information of test cases, *e.g.* coverage information denoted as a statement *executed* or *not executed*, and test results represented as a *passing* or *failing* result. Based on the execution information of test cases, FL approaches apply suspiciousness evaluation algorithms, such as correlation coefficients for SFL or neural networks for DLFL, to rank program statements based on their likelihood of being faulty [17, 18].

Thus, test cases are indispensable for conducting effective fault localization. FL approaches classify test cases into two classes: passing test cases and failing ones, to analyze their distinct behaviors and pinpoint the locations of a fault. However, a significant challenge is the class imbalance between passing and failing test cases, where failing test cases are often severely less in number. This class imbalance can introduce bias into the suspiciousness evaluation [19, 20], and prior research [21] has shown that a more balanced dataset can improve the effectiveness of FL.

Recent research has focused on developing data augmentation approaches for FL that generate balanced test suites to enhance the effectiveness of FL. As modern software systems grow increasingly complex, the dimensionality of the execution information (*e.g.* coverage information regarding the size of a program) of test cases becomes exceedingly high, these data augmentation approaches usually perform dimensionality reduction before data generation. Thus, a typical workflow involves two parts: dimensionality reduction and data generation. Specifically, it first applies

dimensionality reduction techniques to the test cases, followed by data generation approaches to generate new failing test cases until the dataset becomes balanced, where the number of failing test cases is equal to that of passing ones.

In the dimensionality reduction phase, current approaches [10, 11, 12, 13] uses either program slicing [22] or linear dimensionality reduction techniques (*e.g.* linear discriminant analysis [23] and principal component analysis [24]). Despite the promising FL results delivered by these existing approaches, they are still limited. Program slicing focuses on the context of a program based on semantic properties, while linear dimensionality reduction simplifies the dataset based on statistical properties. These approaches, when used separately, can fail to capture both the semantic context of a program and the global statistical information.

In the data generation phase, current approaches can be roughly categorized into traditional transformation approaches and deep learning-based ones. Traditional transformation approaches directly modify failing test cases to generate new ones, *e.g.* Lamont [12] applied SMOTE, and PRAM [11] used a Mixup approach[25] inspired by image augmentation techniques. While effective, these approaches struggle to capture deeper features in the data. To further capture deep features, deep learning-based approaches, *e.g.* generative adversarial networks (GANs[26]) and conditional variational autoencoder (CVAE[27]), train models that learn the characteristics of both passing and failing test cases to generate new failing test cases. [13, 10] have demonstrated the effectiveness of using CVAE and GAN for data augmentation in FL, particularly for DLFL. However, these approaches share a common limitation: both GANs and CVAE consist of two components, *i.e.* GANs with a generator and discriminator, and CVAE with an encoder and decoder. These components are interdependent during training, and the potential for capability mismatches between them can result in unstable sample quality[28].

To address these issues, we propose PCD-DAug : a Principal Context-aware Diffusion guided Data Augmentation approach that generate synthesized failing test cases for improving FL. The basic idea of PCD-DAug is to combines program semantic properties (*i.e.* program slicing) with statistical data properties (*i.e.* principal component analysis) to construct a dimensionality reduced context, and use component-independent deep learning networks (*i.e.* diffusion model) to learn from the context to generate minority class data (*i.e.* failing test cases) for improving FL.

For acquiring a dimensionality reduced context, PCD-DAug uses dynamic program slicing [29] to capture the program semantic properties via program dependencies showing how a set of statements influences the faulty output, and leverages a revised principal component analysis (PCA) [30] to extract global statistical data properties from the coverage data; then embodies the two properties to define a principal context. For generating synthesized failing test cases, PCD-DAug uses the conditional diffusion model [31] to learn the principal context through interdependent components. Unlike GAN and CVAE requiring the training of two interdependent components, diffusion models[32] consist of two processes: a deterministic forward process and a trainable reverse process. The forward process, which progressively adds noise to degrade the original data, is defined by a mathematical formula and requires no training. The training of a model training focuses solely on the reverse process, which learns to progressively denoise the data to recover failing test cases.

It not only avoids the capability mismatch common in GANs and CVAE but also simplifies the training process. By training only the reverse denoising process, we can achieve more efficient and stable generation of failing test cases, ultimately improving FL effectiveness.

To evaluate PCD-DAug , we conducted large-scale experiments on 262 versions across five benchmarks. We applied PCD-DAug to six state-of-the-art FL approaches and compared it with six data augmentation approaches. The experimental results show that PCD-DAug significantly improves the effectiveness of all six FL approaches and outperforms the six data augmentation approaches. For example, compared to the six state-of-the-art FL methods, PCD-DAug improves FL effectiveness by an average of 383.83%, 227.08%, and 224.19% on the Top-1, Top-3, and Top-5 metris, respectively; compared to SOTA of data augmentation approaches, PCD-DAug achieves an improvement of 34.51%, 0.56%, and 3.40% on the same metrics.

The main contributions of this paper can be summarized as follows:

- We propose PCD-DAug : a principal context-aware diffusion guided data augmentation approach integrating principal context with a diffusion model, generating synthesized failing test cases to acquire a class balanced dataset for improving FL.
- We devise a principal context combining program semantic properties (*i.e.* program slicing) with statistical data properties(*i.e.* revised PCA), guiding the data synthesis process within a diffusion model framework.
- We conduct comprehensive experiments involving six state-of-the-art FL techniques, alongside six data augmentation approaches. Our results show that PCD-DAug significantly improves the FL effectiveness.

- We open source the replication package online¹, including the all source codes.

The rest of this paper is structured as follows. Section 2 introduces background information. Section 3 presents our approach PCD-DAug. Section 4 and Section 5 show the experimental results and discussion. Section 6 draws the conclusion.

2 Background

2.1 Diffusion Model

Diffusion models are a type of generative model applied in tasks such as image generation and text-to-image synthesis. In recent years, diffusion models have gained significant attention from researchers due to their impressive performance in both text-to-image and text-to-video generation tasks. A diffusion model consists of two main components: the forward process, also known as the diffusion process, and the reverse process. In the forward process, Gaussian noise is gradually added at each time step to transform the data into a fully noisy result. The reverse process, in turn, works by predicting and removing the Gaussian noise step by step, ultimately recovering the original sample. The detailed processes are as follows:

Forward Process. In the forward process, an original data sample \mathbf{x}_0 undergoes a series of transformations where Gaussian noise is added progressively at each time step. This process is modeled as a Markov chain, and can be described mathematically as follows:

$$\begin{aligned} q(\mathbf{x}_{1:T} | \mathbf{x}_0) &:= \prod_{t=1}^T q(\mathbf{x}_t | \mathbf{x}_{t-1}) \\ q(\mathbf{x}_t | \mathbf{x}_{t-1}) &:= \mathcal{N}(x_t; \sqrt{1 - \beta_t} \mathbf{x}_{t-1}, \beta_t \mathbf{I}) \end{aligned} \quad (1)$$

where x_t represents the data at time step t in the forward process, and x_0 is the original sample. β_t is the variance schedule, which controls the amount of noise added at each step. The variance can either be learned through reparameterization [33] or kept as a constant parameter[32].

As Gaussian noise is continuously added over time, the original sample x_0 is eventually transformed into an indistinguishable noisy version, represented by x_T , which approximates a sample from a standard Gaussian distribution. The forward process transforms the data distribution into a noise distribution. This transformation can also be described mathematically as:

$$x_t = \sqrt{\bar{\alpha}_t} x_0 + \sqrt{1 - \bar{\alpha}_t} \epsilon \quad (2)$$

where $\alpha_t = 1 - \beta_t$ and $\bar{\alpha}_t = \prod_{s=1}^t \alpha_s$. ϵ is the Gaussian-distributed noise.

Reverse Process. The reverse process is designed to recover the original data sample \mathbf{x}_0 from the fully noisy data $\mathbf{x}_T \sim \mathcal{N}(0, \mathbf{I})$. This reverse transformation is achieved through a step-by-step denoising procedure, modeled by a Markov chain. The reverse process can be expressed as:

$$p_{\theta}(\mathbf{x}_{0:T}) = p(\mathbf{x}_T) \prod_{t=1}^T p_{\theta}(\mathbf{x}_{t-1} | \mathbf{x}_t) \quad (3)$$

where $p_{\theta}(\mathbf{x}_{t-1} | \mathbf{x}_t)$ represents the conditional probability of transforming \mathbf{x}_t into \mathbf{x}_{t-1} , which is parameterized as a Gaussian distribution:

$$p_{\theta}(\mathbf{x}_{t-1} | \mathbf{x}_t) = \mathcal{N}(\mathbf{x}_{t-1}; \mu_{\theta}(\mathbf{x}_t, t), \Sigma_{\theta}(\mathbf{x}_t, t)) \quad (4)$$

Where, $\mu_{\theta}(\mathbf{x}_t, t)$ and $\Sigma_{\theta}(\mathbf{x}_t, t)$ are the mean and variance predicted by the model. In most cases, the variance $\Sigma_{\theta}(\mathbf{x}_t, t)$ is set to a constant, and can be defined as:

$$\Sigma_{\theta}(\mathbf{x}_t, t) = \sigma_t^2 \mathbf{I}, \quad \sigma_t^2 = \frac{1 - \bar{\alpha}_{t-1}}{1 - \bar{\alpha}_t} \beta_t \quad (5)$$

As for the mean $\mu_{\theta}(\mathbf{x}_t, t)$, it is computed by removing the noise predicted by the model $\epsilon_{\theta}(\mathbf{x}_t, t)$, and is given by:

¹<https://github.com/sh10f/PCD-DAug>

$$\mu_\theta(\mathbf{x}_t, t) = \frac{1}{\sqrt{\alpha_t}} \left(\mathbf{x}_t - \frac{\beta_t}{\sqrt{1 - \bar{\alpha}_t}} \epsilon_\theta(\mathbf{x}_t, t) \right) \quad (6)$$

In this formulation, $\epsilon_\theta(\mathbf{x}_t, t)$ represents the noise component predicted by the model, which is usually parameterized by a neural network. A commonly used architecture for ϵ_θ is the U-Net [34] or Transformer[35], which allows efficient denoising at each time step.

By iteratively applying this reverse process, the diffusion model progressively removes the Gaussian noise from \mathbf{x}_T , ultimately reconstructing an approximation of the original data \mathbf{x}_0 .

Optimization. The core objective of the diffusion model is to minimize the difference between the noise added during the forward process and the noise predicted during the reverse process. The diffusion model seeks to align the posterior distribution from the forward process with the prior distribution in the reverse process. This alignment is typically achieved by minimizing the Kullback-Leibler (KL) divergence between the two distributions. For simplification, the objective function can be expressed as a mean squared error (MSE) loss between the true noise and the predicted noise:

$$L_{\text{simple}} = \mathbb{E}_{t, \mathbf{x}_0, \epsilon} \left[\left\| \epsilon - \epsilon_\theta \left(\sqrt{\bar{\alpha}_t} \mathbf{x}_0 + \sqrt{1 - \bar{\alpha}_t} \epsilon, t \right) \right\|^2 \right] \quad (7)$$

Here, ϵ represents the Gaussian noise added to the original data sample \mathbf{x}_0 during the forward process, and ϵ_θ is the noise predicted by the model at step t . The goal of training is to minimize the distance between the added noise and the model's predicted noise, thereby learning an effective denoising function.

2.2 Program Slice

Program slicing is a decomposition technique used to extract the parts of a program that directly or indirectly influence the values computed at a specific program point, referred to as the slicing criterion[36, 37]. A slicing criterion typically consists of a pair $\langle p, V \rangle$, where p is a program location, and V is a set of variables of interest. The subset of the program that affects the values of these variables at p is known as the program slice.

This technique analyzes both control dependencies and data dependencies to determine which parts of the program impact the specified point. By isolating these dependencies, program slicing can aid in identifying the source of program failures, providing a more precise, context-aware view for debugging.

Program slicing can be categorized into static slicing and dynamic slicing[29], depending on whether the specific input of the program is considered in the slicing process.

Static program slicing does not take specific program inputs into account. It analyzes all possible execution paths based solely on the program's structure to identify statements that may influence the value of a particular variable. Static slices include all potential paths and are useful for providing a comprehensive analysis of the program's control and data flows, helping developers understand the overall behavior of the program.

Dynamic program slicing is an important technique for debugging, as it includes only the statements along the execution path that affect the value of a variable at a specific program point for a given input. The slicing criterion in dynamic slicing is extended to a triplet $\langle p, V, I \rangle$, where I represents the set of inputs. Dynamic slicing can provide more precise slices by focusing on relevant execution paths, but at the cost of requiring actual program runs.

By comparing the two approaches, dynamic slicing offers more refined results, especially when debugging failures under specific test cases.

3 Approach

This section will introduce our approach PCD-DAug : a Context-Aware and PCA-enhanced Diffusion Model for data augmentation in fault localization. As shown in Figure 1, PCD-DAug operates in three main stages:

PCD-DAug first applies dynamic program slicing to capture the fault semantic context based on the program's structure and data dependencies. Next, by using a revised PCA on the raw data, we extract the statistical context from a statistical analysis perspective. These two contexts are then merged and fed into the training process of the diffusion model, which requires training only the reverse denoising process.

Finally, the trained context-aware diffusion model is used to generate new failing test cases, iteratively synthesizing data until a class-balanced dataset is achieved, where the number of failing test cases matches the passing ones. This class balance significantly improves the performance of fault localization.

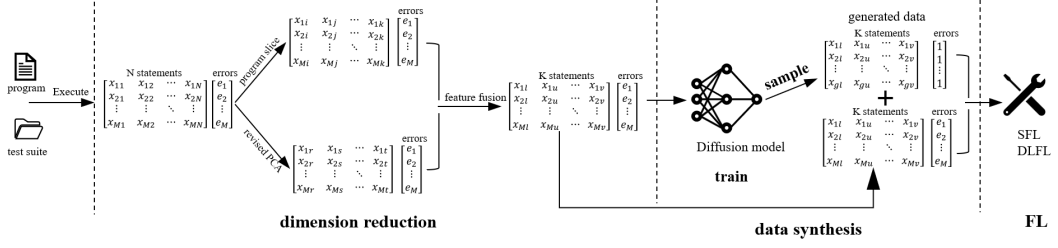


Figure 1: Architecture of PCD-DAug .

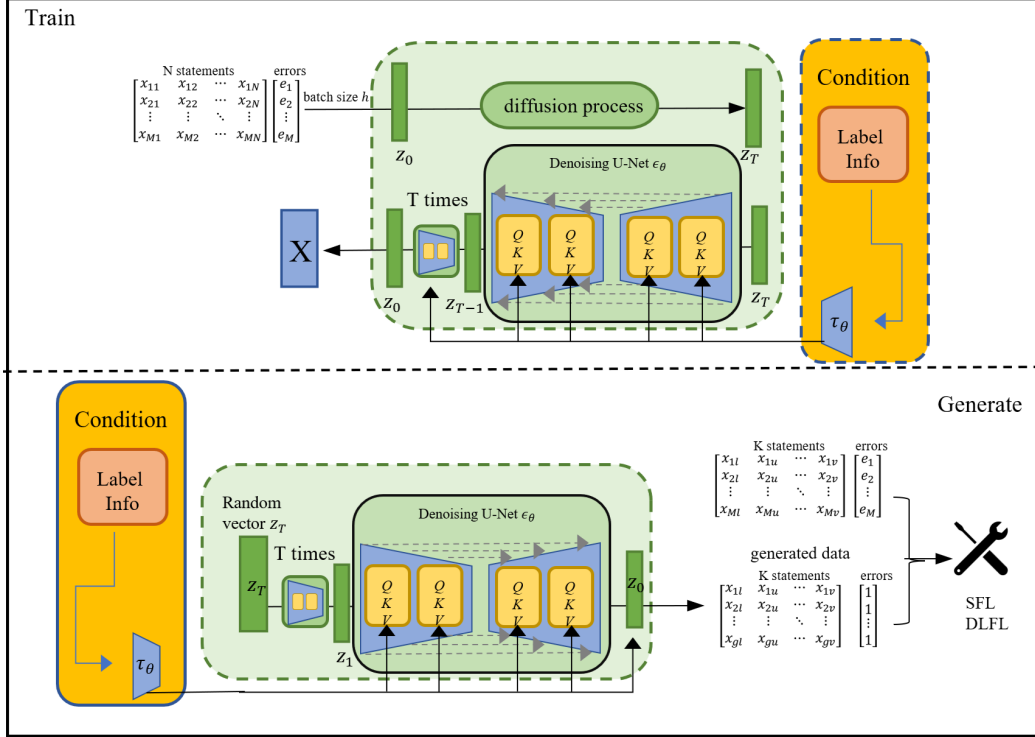


Figure 2: Data synthesis stage of PCD-DAug .

3.1 Fault Semantic Context Construction

The fault semantic context refers to the subset of statements whose execution leads to failing outputs. We employ dynamic program slicing to construct this fault semantic context, as it relies on specific program inputs, aligning with the generation process of the raw data (i.e., the coverage matrix and error vector) in FL. The raw data is derived from runtime information collected when executing the test suite on the program. Furthermore, numerous studies[10, 11] have shown that dynamic program slicing enhances the effectiveness of FL techniques.

To construct the fault semantic context, we define the dynamic program slicing criterion $ScContext$ as:

$$ScContext = (outputStm, outputVar, inputTest) \quad (8)$$

where $outputStm$ represents a point of interest in the program, typically a specific statement. $outputVar$ refers to a set of variables used at $outputStm$. $inputTest$ represents the input to the failing test cases. In previous works [10] and [11], the failing test case with the fewest executed statements was selected for dynamic program slicing to build the context. This approach effectively reduces data dimensionality and focuses attention on a small number of statements, which are most likely to involve single-type faulty statements. However, for more complex programs containing multiple faulty statements or faults of different types, relying on a single failing test case for slicing is

insufficient to capture the complete set of faulty statements. Therefore, we opt to use multiple failing test cases to construct a more comprehensive fault semantic context.

Thus, PCD-DAug generates a new $M \times K'$ context matrix and a new $1 \times K'$ statement index. This context matrix integrates the set of faulty statements responsible for multiple faults by removing duplicate statements across the slices of multiple failing test cases, resulting in a comprehensive and refined representation of the faulty context.

3.2 Statistical Context Construction

Figure 2 illustrates the architecture of our model, in which we use a simplified U-Net to implement the diffusion model. The U-Net architecture includes a single downsampling layer and a single upsampling layer.

However, the fault semantic context only includes a subset of statements derived through dynamic program slicing, capturing structural and data dependencies based on specific inputs. This context is therefore limited to local information tied to particular inputs. To address this limitation, we introduce a revised PCA[30], which not only retains the statistical properties of the data but also enriches the context by incorporating statistical dependencies, complementing the structural information obtained from program slicing. Through this fusion, we ensure that the context aligns with the model's dimensional requirements.

Algorithm 1 describes feature selection using revised PCA. It takes the coverage matrix X , the statement set $StmSC$ from program slicing, and two key parameters: the *number of largest eigenvalues* m and *number of principal components* K'' .

It firstly computes the covariance matrix $covX$, solves for eigenvalues and eigenvectors, and selects the top m eigenvectors (Steps 1-4).

Contribution values c_i are calculated by summing the m elements in each row of matrix V , and the top indices are stored in $iContriMax$ (Steps 6-8).

Finally, it generates the statistical context matrix X_{PCA} of size $M \times K''$ and context index vector $StmPCA$ by selecting columns from X corresponding to $iContriMax$, and returns X_{PCA} and $StmPCA$ (Steps 9-14).

Algorithm 1: dimensionality reduction using revised PCA

Input:

coverage matrix with the size of $M \times N$: X ,
number of largest eigenvalues: m ,
number of principal components: K''

Output:

statistical context matrix with size of $M \times K''$: X_{PCA}
statistical context index with size of $1 \times K''$: $StmPCA$
 $covX$ = covariance matrix of original samples;
 $eigenVec$ = eigenvectors of $covX$;
 $eigenVal$ = eigenvalues of $covX$;
 V = select the $eigenVec$ corresponding to the first m largest $eigenVal$;
for $i = 1$ **to** N **do**
 | Calculate contribution value: $c_i = \sum_{p=1}^m |V_{pi}|$;
 $iContriMax = \text{argmax}(c)$;
Initialize X_{PCA} and $StmPCA$ as None, None;
for $i = 1$ **to** K'' **do**
 | Add the $iContriMax[i]$ -th column of X to X_{PCA} ;
 | Add $iContriMax[i]$ to $StmPCA$;
return X_{PCA} , $StmPCA$;

3.3 Context-aware Diffusion Model

Algorithm 2 describes the fusion process, which integrates semantic and statistical contexts to refine the coverage matrix. The inputs include the coverage matrix X , the statement index $StmSC$ from program slicing, the statistical context index $StmPCA$, and a fusion ratio α .

Algorithm 2: Context Fusion Using Fault Semantic and Statistical Contexts**Input:**

coverage matrix with the size of $M \times N$: X ,
 statements index selected by program slicing with the size of $1 \times K'$: $StmSC$,
 statistical context index with size of $1 \times K''$: $StmPCA$,
 fusion ratio: α

Output:

reduced coverage matrix with size of $M \times K$: X_{fusion}
 Set fusion size as $K^f = \alpha \times K'$;
 Set fusion context statements index $StmFusion = StmSC \cap StmPCA[:K^f]$;

for $i = 1$ **to** K'' **do**

if $StmFusion$ matches the dimensional requirements of PCD-DAug or DLFL **then**
 break;
 if $StmPCA[i] \notin StmFusion$ **then**
 if $StmPCA[i] \in StmSC$ **then**
 add $StmPCA[i]$ to $StmFusion$;

Initialize reduced coverage matrix X_{fusion} as None;

for $i = 1$ **to** $len(StmFusion)$ **do**

add $StmFusion[i]$ – th column of X to X_{fusion} ;

return X_{fusion} ;

The algorithm first calculates the fusion size K^f as $\alpha \times K'$ and initializes $StmFusion$ as the intersection of $StmSC$ and the top K^f elements of $StmPCA$ (Steps 1-2).

Next, it iterates through $StmPCA$ to expand $StmFusion$ as needed. If an element in $StmPCA$ is also in $StmSC$ but not yet in $StmFusion$, it is added to $StmFusion$ (Steps 3-7). This ensures that essential statements from both contexts are included.

Finally, X_{fusion} is constructed by selecting columns from X based on $StmFusion$, and X_{fusion} is returned (Steps 8-12).

In fault localization, high-quality data augmentation must reflect the specific program contexts most relevant to causing failures. Randomly generated failing data can introduce noise, which may hinder the model’s ability to effectively localize faults. To ensure that the generated data remains aligned with the original failure-inducing conditions, we explore two possible guidance strategies: classifier-based guidance and classifier-free guidance.

3.3.1 Classifier-Based Strategy

To guide sample generation in the reverse diffusion process, we leverage gradients of the target data distribution. [38] adding a classifier gradient to the noise term can direct sample generation toward specific target classes. This approach modifies the noise prediction equation as follows:

$$\hat{\epsilon} = \epsilon_\theta(\mathbf{x}_t) - \gamma \cdot \sqrt{1 - \bar{\alpha}t} \nabla \mathbf{x}_t \log p_\phi(y|\mathbf{x}_t) \quad (9)$$

where γ controls the level of guidance, and $p_\phi(\cdot)$ represents the classifier’s probability function.

3.3.2 Classifier-Free Strategy

In fault localization, relying on a pre-trained classifier introduces extra computational cost, particularly in complex and high-dimensional program data.

To mitigate this, we adopt a classifier-free approach for guidance[31], which retains effective sample generation without depending on an external classifier. This alternative strategy redefines the noise prediction in the reverse process as:

$$\hat{\epsilon} = (1 + \gamma) \cdot \epsilon_\theta(\mathbf{x}_t, t, \mathbf{c}) - \gamma \cdot \epsilon_\theta(\mathbf{x}_t, t) \quad (10)$$

where γ again serves as the guidance scale, offering control over the generation direction without requiring pre-trained classifier involvement.

3.3.3 Sampling with DPM-Solver

To further improve the efficiency of the diffusion process in our fault localization model, we employ the DPM-Solver sampler [39]. DPM-Solver is a fast, high-order solver specifically designed for diffusion ODEs, with guaranteed convergence order. It is suitable for both discrete-time and continuous-time diffusion models without requiring any further training. Experimental results demonstrate that DPM-Solver can generate high-quality samples with only 10 to 20 function evaluations across various datasets in Computer Vision.

In our model, we set the sampling steps to **25**. DPM-Solver significantly reduces sampling time while maintaining high sample quality. It solves the probability flow ordinary differential equation (ODE) that governs the diffusion process, approximating the reverse process as follows:

$$d\mathbf{x}(t) = \epsilon_\theta(t) \left(\frac{\mathbf{x}(t)}{\sqrt{\sigma^2 + 1}} \right) d\sigma(t) \quad (11)$$

where σ_t is the noise schedule parameterized by $\sqrt{1 - \alpha_t} / \sqrt{\alpha_t}$, and $\mathbf{x}(t)$ represents the latent state at time t . This method allows our fault localization model to efficiently generate failure-related samples with minimal computational overhead, making it scalable for large program datasets with high-dimensional inputs, especially when using classifier-free guidance.

3.4 Model Training

After merging the fault semantic context with the statistical context, we obtain a $M \times K$ context matrix derived from the $M \times N$ raw data. This context matrix captures the information related to the statements that lead to program failures, combining insights from both the program's structure and statistical analysis. PCD-DAug uses this context matrix as input to the diffusion model, which generates synthesized failing test cases. The diffusion model learns the characteristics of both failing and passing test cases through its forward and reverse processes, ensuring that the newly synthesized samples reflect the key patterns present in the raw data.

In the forward process, PCD-DAug gradually adds Gaussian noise to the original context matrix over multiple time steps, following a classifier-free guidance strategy. In the reverse process, PCD-DAug predicts the noise at each step using the trained model and gradually denoises the noisy data to recover the synthesized samples. The reverse process is trained using a mean squared error (MSE) loss function to minimize the difference between the added noise and the predicted noise.

As shown in Figure 2, the diffusion model, once trained, generates new failing test cases by sampling from noise using DPM-Solver, while also incorporating label information to ensure the synthesized samples reflect the failure characteristics of the original test cases. The newly generated failure samples are then combined with the passing data to form a balanced dataset, which is used to enhance the performance of fault localization methods such as SFL and DFL.

3.5 An Illustrative Example

To illustrate the workflow of PCD-DAug, we provide an example in Figure 3. Here, program P contains 16 statements with a fault at line 3, where the value 0 is mistakenly set instead of 6. The SFL method GP02 [40] is applied to locate the faulty statement.

Each cell below a statement indicates its execution by a test case (0 if not executed, 1 if executed). The 'result' column in Figure 1 shows test outcomes (1 for failure, 0 for success). The original test suite is imbalanced, with four passing test cases (t_1, t_2, t_4, t_5) and two failing cases (t_3, t_6).

To balance this dataset, PCD-DAug generates two additional failing test cases. Program slicing is applied to extract fault semantic context from t_3 and t_6 . Using Eq. (8), we define $(S_{14}, d1, t_3)$ and $(S_{15}, d2, t_6)$ as slicing criteria, given the incorrect output of variable $d1$ at S_{14} during t_3 . As shown in Figure 3, the $StmSC$ matrix for t_3 includes $\{S_1, S_3, S_7, S_{14}\}$ and for t_6 includes $\{S_1, S_3, S_8, S_{15}\}$. So the fault semantic context contains $\{S_1, S_3, S_7, S_8, S_{14}, S_{15}\}$. Revised PCA yields the $StmPCA$ matrix $\{S_{14}, S_{15}, S_{10}, S_{11}, S_6, S_1, S_2, S_3, S_{13}, S_4, S_5, S_{16}, S_8, S_7, S_9, S_{12}\}$. With a fusion ratio α set to 1, the fusion size K^f is equal to $StmSC$. Fusing the fault semantic context and statistical context forms the context $\{S_1, S_3, S_{14}, S_{15}\}$.

Using this enriched context, PCD-DAug employs a Diffusion Model to generate synthetic failing test cases (t_7 and t_8), highlighted in yellow in Figure 3. These new cases expand the context matrix, allowing GP02 to re-evaluate statement suspiciousness with updated data.

Program															Bug information					
S1:Read(a,b,c) S2:d1=0,d2=0,d3=0 S3:if(b < 0){ S4:d1 = b; S5:d2 = c; S6:d3 = a;} S7:else {d1 = b+1;	S8: d2 = c+1; S9:if(a < 0){ S10:a = a+c;} S11: else a = a+b; S12: d3 = a+1;} S13:if(c>0){ S14:output(d1);}	S15:else {output(d2); S16:output(d3);}	t7 and t8 are new failing tests generated by CPDM. Program Slice result: {s1,s3,s7,s8,s14,s15}															S3 is faulty. Correct form: if(b<6){		
test	a,b,c	S1	S2	S3	S4	S5	S6	S7	S8	S9	S10	S11	S12	S13	S14	S15	S16	result		
t1	5,-6,-8	1	1	1	1	1	1	0	0	0	0	0	0	1	0	1	1	0	1	0
t2	4,7,11	1	1	1	0	0	0	1	1	1	0	1	1	1	0	0	0	0	0	0
t3	-1,5,3	1	1	1	0	0	0	1	1	1	1	0	1	1	1	0	0	1	0	1
t4	-2,-7,5	1	1	1	1	1	1	0	0	0	0	0	0	1	1	0	0	0	0	0
t5	-5,8,-8	1	1	1	0	0	0	1	1	1	1	0	1	1	0	1	1	1	0	0
t6	4,2,-1	1	1	1	0	0	0	1	1	1	0	1	1	1	0	1	1	1	1	1
t7		1	1	1												1	0		1	
t8		0		<u>1</u>												1	0		1	
GP02	susp	1.0	1.0	1.0	0.5	0.5	0.5	0.25	0.25	0.25	0.0	0.5	0.25	1.0	0.0	4.0	4.0	-		
	rank	3	4	<u>5</u>	7	8	9	11	12	13	15	10	14	6	16	1	2	-		
GP02 (CPDM)	susp	1.8		4.0												4.5	0.2		-	
	rank	3		<u>2</u>												1	4		-	

Figure 3: An example illustrating PCD-DAug .

The final rows of Figure 3 compare FL results from GP02 with and without PCD-DAug . Without PCD-DAug , GP02 ranks the statements (highlighted in green) as $\{S_{15}, S_{16}, S_1, S_2, S_3, S_{13}, S_4, S_5, S_6, S_{11}, S_7, S_8, S_9, S_{12}, S_{10}, S_{14}\}$. After applying PCD-DAug , the ranking shifts to $\{S_{14}, S_3, S_1, S_{15}\}$. Notably, the faulty statement S_3 moves from 5th to 2th, demonstrating PCD-DAug 's effectiveness in mitigating class imbalance and enhancing fault localization accuracy.

4 Experiments

To assess the effectiveness of our proposed approach, we carried out experiments on 262 versions of five representative benchmark programs, all of which contain real-world faults. The selected programs—Chart, Math, Lang, Time, and Mockito—were drawn from the Defects4J² dataset[41]. Due to the substantial size of these programs, manually collecting input data would be highly time-consuming. Consequently, we leveraged the coverage matrix provided by Pearson et al.[42] to optimize and expedite the experimental process.

Table 1 provides an overview of the five subject programs. For each program, it includes a brief functional description (in the 'Description' column), the number of faulty versions available (in the 'Versions' column), the program size measured in thousand lines of code (in the 'LoC(K)' column), and the number of test cases (in the 'Tests' column).

Table 1: Subject programs

Programs	Description	Versions	Loc(K)	Tests
Chart	Java chart library	26	96	2205
Lang	Apache commons-lang	65	22	2245
Math	Apache commons-math	106	85	3602
Time	Standard date and time library	27	28	4130
Mockito	Mocking framework for Java	38	67	1075
Total	-	262	298	13257

²<https://github.com/rjust/defects4j>

4.1 Experiment Settings

The experiments were conducted on a Linux server equipped with 40 cores of a 2.4GHz CPU and 252GB of RAM. The operating system used was Ubuntu 20.04.

Table 2 provides the main parameters used in our experiments. Notably, we applied this same set of hyper-parameters across 262 faulty versions of the programs, effectively treating each version as a unique dataset. This set demonstrates the robustness and adaptability of our approach and parameter configuration, as it performs consistently well across diverse fault scenarios.

Table 2: Main Parameters of PCD-DAug

Main Parameters	Description	Value
steps	Number of diffusion steps	1000
lr	Learning rate	0.0003
op	Optimizer	AdamW
β_1	Initial value of beta in the diffusion process	0.0001
β_T	Final value of beta in the diffusion process	0.02
α	Fusion ratio in context fusion	1

4.2 Evaluation Metrics

We employ four widely recognized metrics in FL to evaluate the performance of our approach:

- **Number of Top-K:** It quantifies the number of faulty versions where at least one fault is ranked within the top K positions by a fault localization (FL) method. Following the prior work[17, 4], we assign K with the value of 1, 3 and 5 for our evaluation.
- **Mean Average Rank (MAR)[4]:** For each faulty version, we calculate the average rank of all faulty statements in the ranking list. A lower value of MAR indicates better FL effectiveness.
- **Mean First Rank (MFR)[4]:** MFR determines the rank of the first located faulty statement for each version and computes the mean rank across all versions.
- **Relative Improvement (RIMp)[9]:** This metric evaluates the efficiency of fault localization methods by comparing the number of statements that must be examined. RIMp specifically reflects the proportion of statements examined when using our method in comparison to others, where a lower RIMp value indicates superior performance.

These metrics offer a thorough evaluation of our approach’s fault localization accuracy, allowing for performance comparisons with other fault localization methods.

4.3 Research Questions and Results

We evaluate the effectiveness of our approach through the following four research questions.

RQ1. How effective is PCD-DAug in localizing real faults compared with original state-of-the-art SFL methods?

We assessed the performance of three statement-level SFL methods (Dstar[8], Ochiai[43], and Barinel[44]) under two different conditions: the original SFL method and our approach PCD-DAug version. These original methods typically process raw data without any additional context. The results for Top-1, Top-3, Top-5, MFR, and MAR metrics are summarized in Table 3, offering a comparison between the original methods and our approach PCD-DAug .

Top-K. As shown in Table 3, PCD-DAug demonstrates a clear advantage in Top-K metrics across different program datasets, with particularly strong performance on the Lang dataset. In the Top-1, Top-3, and Top-5 rankings, PCD-DAug identified 11, 19, and 27 faults on average using three SFL methods (Dstar, Ochiai, and Barinel), compared to 5, 17, and 24 faults identified by the original methods. This represents performance improvements of 120%, 11.76%, and 12.5%, respectively, indicating that the hyper-parameters used in PCD-DAug were especially effective for the Lang dataset.

In other datasets, PCD-DAug generally outperforms the original methods as well. For instance, in the Math dataset, PCD-DAug shows a slight average improvement across all Top-K metrics. However, on the Mokito dataset, PCD-DAug ‘s performance in Top-3 metrics slightly lags behind the original methods. Specifically, the average number of faults

Table 3: The results of TOP-1, TOP-3, TOP-5, MFR and MAR by comparison of original SFL method and **PCD-DAug**

Program	Scenario	Top-1			Top-3			Top-5			MFR			MAR		
		Dstar	Ochiai	Barinel	Dstar	Ochiai	Barinel	Dstar	Ochiai	Barinel	Dstar	Ochiai	Barinel	Dstar	Ochiai	Barinel
Chart	Origin	3	3	2	7	7	6	10	10	10	305.74	189.26	138.13	322.49	206.93	152.35
	PCD-DAug	3	3	1	7	8	7	9	9	10	116.25	116.46	66.00	125.19	125.31	72.30
Lang	Origin	5	5	5	17	17	17	24	24	24	29.14	30.45	33.17	81.61	60.41	61.48
	PCD-DAug	12	12	10	19	19	21	27	28	28	19.00	18.78	23.00	27.67	27.67	29.32
Math	Origin	17	17	17	32	32	31	38	39	39	59.84	61.35	68.24	315.93	209.81	212.46
	PCD-DAug	18	15	18	32	32	30	40	39	40	65.48	66.02	64.04	98.97	99.74	93.07
Time	Origin	2	2	2	10	10	9	10	10	10	398.63	598.96	600.78	675.20	874.50	875.55
	PCD-DAug	3	3	1	8	7	8	10	10	10	125.89	126.74	135.78	137.04	137.53	143.47
Mokito	Origin	5	6	4	11	11	8	12	12	10	276.86	220.06	230.08	461.74	417.09	420.42
	PCD-DAug	5	5	6	8	9	8	12	12	10	94.39	92.29	90.71	132.01	129.91	125.49
Total	Origin	32	33	30	77	77	71	94	95	93	140.07	143.69	144.24	315.42	270.63	267.69
	PCD-DAug	41	38	36	74	75	74	98	98	98	69.05	69.01	65.31	92.35	92.41	85.19

identified in the Top-3 rankings decreased by 16.67%, respectively. This may be due to the hyper-parameters being optimized for the Lang dataset, without further adjustment for the specific characteristics of other datasets, which could have led to a slight performance trade-off on certain datasets.

Overall, PCD-DAug exhibits consistent performance gains across all SFL methods in Top-1 and Top-5 metrics. For example, using the Barinel method, PCD-DAug correctly identified 36, 74, and 98 faults in the Top-1, Top-3, and Top-5 rankings, compared to 30, 71, and 93 faults identified by the original Barinel method. This corresponds to improvements of 20.00%, 4.23%, and 5.38%, respectively. These results demonstrate that PCD-DAug not only performs well on individual datasets but also shows superior average performance across all datasets, validating its effectiveness in improving fault localization accuracy.

Furthermore, the use of unified hyper-parameters brings important advantages to the application of PCD-DAug. First, it simplifies the model deployment process by eliminating the need to tune hyper-parameters for each individual dataset, thereby enhancing the model's generality. Second, using a unified hyper-parameter setting helps reduce the risk of overfitting, contributing to greater stability and consistency in model performance. Finally, this unified configuration enhances the reproducibility of experimental results and allows for better performance comparison across datasets.

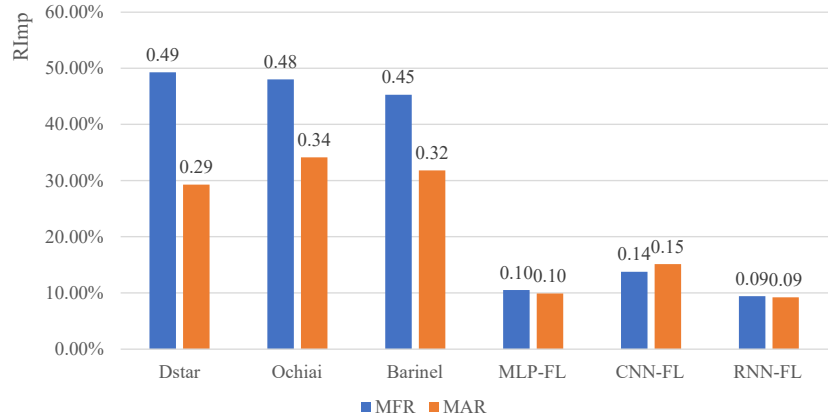


Figure 4: The RImp of MFR and MAR for PCD-DAug over six original FL methods.

RImp. In Figure 4, the RImp values across the evaluated SFL methods (Dstar, Ochiai, and Barinel) consistently remain below 100%, demonstrating that PCD-DAug outperforms these traditional techniques in fault localization efficiency. For example, as depicted in Figure 4, PCD-DAug significantly reduces the MFR metric across the SFL methods. When using PCD-DAug, the percentage of statements that need to be inspected to find first faulty statement ranges from 45.28% with Barinel to 49.29% with Dstar. This implies that PCD-DAug can reduce the number of statements required for examination by 50.71% ($100\% - 49.29\% = 50.71\%$) for Dstar and 54.72% ($100\% - 45.28\% = 54.72\%$) for Barinel. Thus, our approach PCD-DAug can lead to substantial reductions in the effort required for fault localization.

Summary for RQ1: In RQ1, we evaluated the performance of PCD-DAug against three traditional SFL methods. The findings show that PCD-DAug achieves better results compared to the original methods, indicating that PCD-DAug provides a more effective approach for fault localization.

RQ2. How effective is PCD-DAug in localizing real faults compared with the state-of-the-art DLFL methods?

Table 4: The results of TOP-1, TOP-3, TOP-5, MFR and MAR by comparison of original DLFL method and **PCD-DAug**

Program	Scenario	Top-1			Top-3			Top-5			MFR			MAR		
		MLP-FL	CNN-FL	RNN-FL	MLP-FL	CNN-FL	RNN-FL	MLP-FL	CNN-FL	RNN-FL	MLP-FL	CNN-FL	RNN-FL	MLP-FL	CNN-FL	RNN-FL
Chart	Origin	1	0	2	3	0	3	4	0	3	609.22	560.22	848.78	807.25	649.92	967.27
	PCD-DAug	5	1	3	8	1	6	10	3	9	63.21	158.79	68.58	68.07	178.46	86.08
Lang	Origin	3	0	0	8	1	2	13	2	4	196.43	390.43	331.34	289.21	442.95	442.47
	PCD-DAug	13	7	8	20	11	15	28	19	25	18.92	23.00	26.51	30.55	33.84	30.27
Math	Origin	1	2	0	10	2	3	12	2	6	526.78	1104.67	950.20	978.65	1190.07	1316.76
	PCD-DAug	19	5	6	31	11	14	36	16	22	64.89	118.63	70.63	102.27	152.97	103.28
Time	Origin	0	0	0	0	0	0	0	0	0	2228.56	2603.96	1627.07	2756.34	2809.59	2211.87
	PCD-DAug	1	0	1	2	0	2	5	0	3	129.15	460.63	173.14	162.22	508.83	198.90
Mokito	Origin	0	0	0	0	0	0	0	1	0	527.44	811.97	578.86	808.75	1005.73	890.16
	PCD-DAug	4	0	3	6	2	4	8	4	5	107.11	136.26	109.58	149.02	182.05	149.83
Total	Origin	5	2	2	21	3	8	29	5	13	629.49	991.81	803.70	951.90	1097.09	1098.64
	PCD-DAug	42	13	21	67	25	41	87	42	64	66.08	136.52	75.81	94.24	165.85	101.07

In addition to comparing PCD-DAug with the original SFL methods, we also evaluated its performance against three representative DLFL approaches: MLP-FL[16], CNN-FL[9], and RNN-FL[15]. As shown in Table 4, PCD-DAug consistently outperforms these methods across all Top-K metrics.

Top-K. For example, in comparison with MLP-FL, PCD-DAug located 42, 67, and 87 faults in the Top-1, Top-3, and Top-5 metrics, respectively, while MLP-FL only identified 5, 21, and 29 faults in these categories. This represents substantial improvements of 740.00%, 219.05%, and 200.00% in Top-1, Top-3, and Top-5 metrics, respectively, for PCD-DAug over the original MLP-FL method.

RImp. Furthermore, PCD-DAug achieves lower mean first rank (MFR) and mean average rank (MAR) values compared to all baseline DLFL methods, indicating a more efficient fault localization process. As illustrated in Figure 4, the RI^{mp} values for MFR reveal that PCD-DAug significantly reduces the number of statements requiring inspection. With PCD-DAug, the statements needing examination range from 9.43% (for RNN-FL) to 13.76% (for CNN-FL), corresponding to reductions of 86.24% ($100\% - 13.76\% = 86.24\%$) to 90.57% ($100\% - 9.43\% = 90.57\%$) in comparison to the original DLFL approaches.

Similarly, for the MAR metric, PCD-DAug reduces the number of statements to be examined to between 9.20% (for RNN-FL) and 15.12% (for CNN-FL), translating to reductions of 84.88% ($100\% - 15.12\% = 84.88\%$) to 90.80% ($100\% - 9.20\% = 90.80\%$). These results demonstrate PCD-DAug's substantial efficiency gains, significantly minimizing the fault localization effort compared to the original DLFL methods.

Summary for RQ2: In RQ2, we analyzed the performance of PCD-DAug against three DLFL methods. The result reveals that PCD-DAug consistently outperforms these methods across most metrics. These findings demonstrate that PCD-DAug is more effective at fault localization compared to the state-of-the-art DLFL methods.

RQ3. How effective is PCD-DAug in localizing real faults compared with the data optimization FL methods?

In addition to comparing PCD-DAug with the original SFL and DLFL methods, we evaluated its performance against two widely-used data optimization techniques: undersampling[45] and resampling[46, 47, 48]. As shown in Table 5, PCD-DAug consistently outperforms both optimization methods across all Top-K metrics. For example, using the Barinel fault localization method, PCD-DAug located 36, 74, and 98 faults in the Top-1, Top-3, and Top-5 metrics, respectively. In comparison, the undersampling method identified only 15, 40, and 62 faults, while the resampling method located 29, 68, and 89 faults. This translates to PCD-DAug achieving improvements of 106.67%, 85.00%, and 58.06% over undersampling for the Top-1, Top-3, and Top-5 metrics, respectively, and surpassing resampling by 24.14%, 8.82%, and 10.11% in these same metrics. These results highlight PCD-DAug's enhanced fault localization effectiveness over both data optimization techniques.

Moreover, in terms of the MFR and MAR metrics, PCD-DAug achieves lower values than both the undersampling and resampling methods, indicating that it ranks faulty statements higher on average and requires fewer statements to be inspected to locate faults. This efficiency in fault localization is further supported by the RI^{mp} values, as shown in Figure 5 and Figure 6. All RI^{mp} values are below 100%, indicating that PCD-DAug requires fewer statements to be examined than either undersampling or resampling.

Table 5: Comparisons between PCD-DAug and two data optimization methods for TOP-1, TOP-3, TOP-5, MAR, and MFR.

FL	Scenario	Top-1	Top-3	Top-5	MFR	MAR
Dstar	Undersampling	16	42	62	185.08	346.63
	Resampling	28	66	82	154.68	325.00
	PCD-DAug	41	74	98	69.05	92.35
Ochiai	Undersampling	16	42	62	187.27	327.63
	Resampling	28	66	82	156.41	279.12
	PCD-DAug	38	75	98	69.01	92.41
Barinel	Undersampling	15	40	62	175.89	308.74
	Resampling	29	68	89	140.76	256.50
	PCD-DAug	36	74	98	65.31	85.19
MLP-FL	Undersampling	20	47	63	230.83	493.45
	Resampling	33	67	84	244.83	539.48
	PCD-DAug	42	67	87	66.08	94.24
CNN-FL	Undersampling	1	6	9	997.39	1123.55
	Resampling	1	2	4	845.84	1002.27
	PCD-DAug	13	25	42	136.52	165.85
RNN-FL	Undersampling	2	14	29	362.07	639.37
	Resampling	13	30	47	275.63	464.28
	PCD-DAug	21	44	64	75.81	101.07

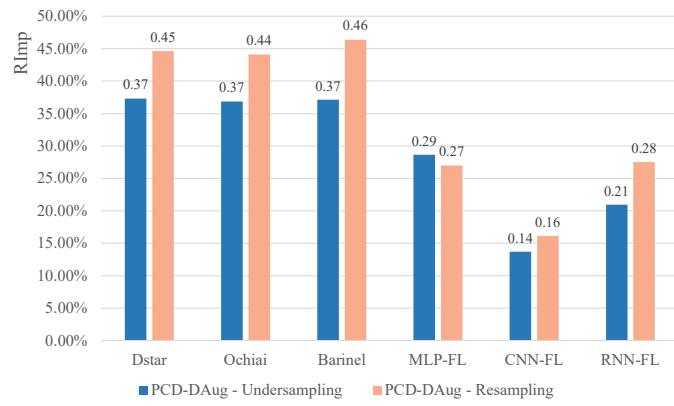


Figure 5: The RImp of MFR by PCD-DAug over two data optimization methods.

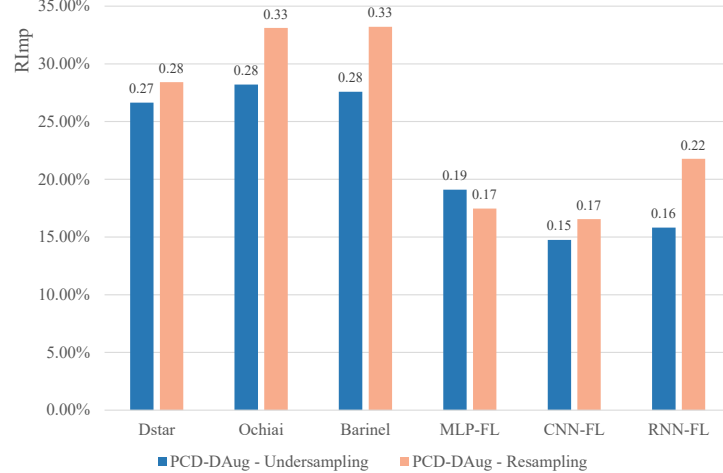


Figure 6: The RImp of MAR by PCD-DAug over two data optimization methods.

Specifically, for the MFR metric, PCD-DAug reduces the number of statements that need to be examined to between 13.69% (for CNN-FL) and 37.31% (for Dstar) compared to undersampling, equating to reductions of 62.69% (100% – 37.31%) to 86.31% (100% – 13.69%). When compared to resampling, PCD-DAug reduces the statements to be examined to between 16.14% (for CNN-FL) and 46.40% (for Barinel), corresponding to reductions of 53.60% (100% – 46.40%) to 83.86% (100% – 16.14%).

Similarly, for the MAR metric, PCD-DAug consistently requires fewer statements to be inspected across all six fault localization methods compared to both undersampling and resampling. PCD-DAug reduces the average number of statements that need to be examined to between 14.76% (for CNN-FL) and 28.21% (for Ochiai) compared to undersampling, equating to reductions of 71.79% (100% – 28.21%) to 85.24% (100% – 14.76%). When compared to resampling, PCD-DAug reduces the statements to be examined to between 16.55% (for CNN-FL) and 33.11% (for Ochiai), corresponding to reductions of 76.89% (100% – 33.11%) to 83.45% (100% – 16.55%). This significant reduction in the number of statements inspected demonstrates PCD-DAug’s consistent advantage in minimizing the fault localization effort. These findings collectively validate the superior effectiveness and efficiency of PCD-DAug in fault localization tasks.

Summary for RQ3: In RQ3, we evaluated the performance of PCD-DAug against two data optimization techniques. The analysis shows that PCD-DAug surpasses both undersampling and resampling in terms of fault localization, with improvements observed across most metrics. This demonstrates that PCD-DAug is a more effective approach for fault localization compared to these optimization methods.

RQ4. How effective is PCD-DAug in localizing real faults compared with four state-of-the-art data augmentation methods?

In addition to comparing PCD-DAug with data optimization methods, we also evaluated its performance against four data augmentation approaches: Aeneas [13], Lamont [12], CGAN4FL [10], and PRAM [11].

As shown in Table 6, PCD-DAug consistently outperforms the other data augmentation methods across all cases based on Top-K metrics and the MFR and MAR rankings except for CGAN4FL in CNN-FL on Top-3 metric and PRAM in RNN-FL. Specifically, PCD-DAug achieves higher fault identification rates at Top-1, Top-3, and Top-5 levels across all fault localization (FL) methods. For instance, in the Barinel method, PCD-DAug identified 36, 74, and 98 faults at the Top-1, Top-3, and Top-5 levels, respectively, outperforming CGAN4FL (28, 55, 66) and PRAM (30, 74, 97). This translates to improvements of 28.57%, 34.55%, and 48.48% over CGAN4FL, and 20.00%, 0.00%, and 2.06% over PRAM, demonstrating a significant increase in fault localization accuracy.

PCD-DAug’s advantage also extends to efficiency metrics. In terms of Mean First Rank (MFR) and Mean Average Rank (MAR), PCD-DAug shows consistently lower scores across all FL methods, indicating that it requires fewer statements to be examined. For example, in the Barinel method, PCD-DAug’s MFR is 65.31, significantly lower than CGAN4FL’s 89.38 and PRAM’s 73.41, which indicates faster fault detection. In the MAR metric, PCD-DAug also performs well; for instance, in the CNN-FL method, PCD-DAug achieves a MAR of 165.85, much lower than PRAM’s

Table 6: Comparisons between PCD-DAug and four data augmentation methods for TOP-1, TOP-3, TOP-5, MAR, and MFR.

FL	Scenario	Top-1	Top-3	Top-5	MFR	MAR
Dstar	Aeneas	12	31	39	489.19	657.84
	Lamont	31	61	74	294.93	495.04
	CGAN4FL	35	72	87	78.44	109.18
	PRAM	30	74	99	73.38	93.06
	PCD-DAug	41	74	98	69.05	92.35
Ochiai	Aeneas	30	56	70	462.96	647.84
	Lamont	31	61	73	279.83	449.67
	CGAN4FL	34	70	83	94.73	130.45
	PRAM	31	75	98	72.56	96.12
	PCD-DAug	38	75	98	69.01	92.41
Barinel	Aeneas	18	38	50	475.02	656.98
	Lamont	30	60	74	265.61	441.02
	CGAN4FL	28	55	66	89.38	116.50
	PRAM	30	74	97	73.41	96.69
	PCD-DAug	36	74	98	65.31	85.19
MLP-FL	Aeneas	8	24	32	477.75	655.15
	Lamont	27	60	79	341.09	614.91
	CGAN4FL	31	58	67	100.86	144.63
	PRAM	24	65	80	68.35	106.70
	PCD-DAug	42	67	87	66.08	94.24
CNN-FL	Aeneas	1	7	12	516.34	691.63
	Lamont	1	2	4	691.87	905.89
	CGAN4FL	2	26	39	170.08	197.94
	PRAM	5	24	32	173.92	221.50
	PCD-DAug	13	25	42	136.52	165.85
RNN-FL	Aeneas	2	6	11	489.77	673.54
	Lamont	9	26	33	399.58	665.69
	CGAN4FL	15	32	45	101.60	142.19
	PRAM	22	45	65	95.69	132.16
	PCD-DAug	21	44	64	75.81	101.07

221.50. This demonstrates that PCD-DAug not only improves fault localization accuracy but also reduces the effort needed for locating faults.

Figure 7 and Figure 8 further illustrate PCD-DAug 's relative improvement (RImp) o

ver Aeneas, Lamont, CGAN4FL, and PRAM in both MFR and MAR metrics across six different FL methods. In all cases, the RImp values are below 100%, indicating that PCD-DAug requires fewer statements to be examined than other data augmentation methods. Specifically, for the MFR metric, PCD-DAug reduces the number of statements to be examined to between 78.50% (for CNN-FL) and 95.11% (for Ochiai) compared to PRAM, representing reductions of 4.89% (100% – 95.11%) to 21.50% (100% – 78.50%).

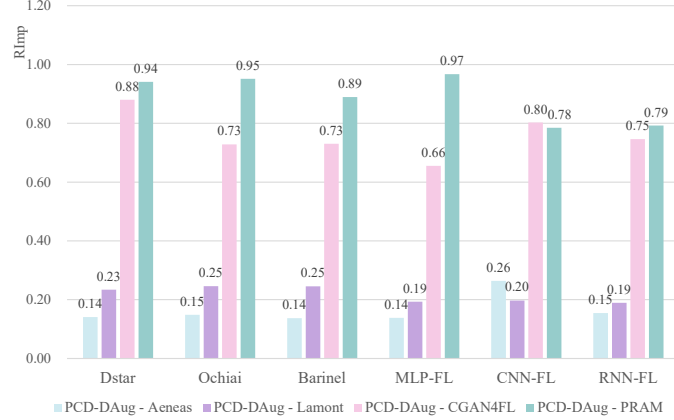


Figure 7: The RImp of MFR by PCD-DAug over four data augmentation methods.

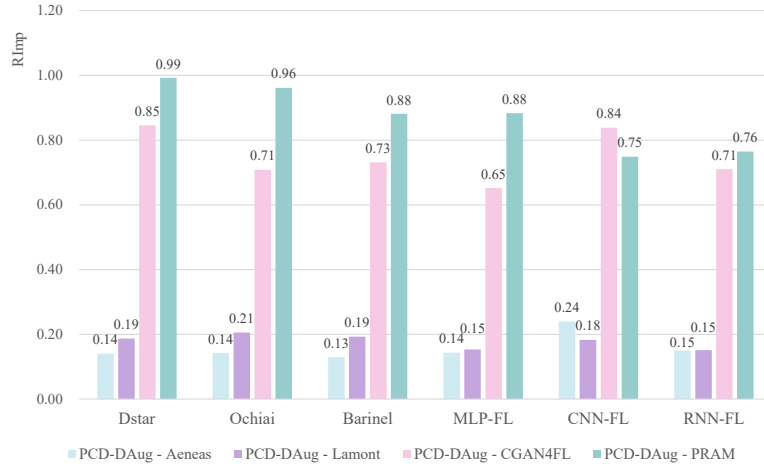


Figure 8: The RImp of MAR by PCD-DAug over four data augmentation methods.

Similarly, for the MAR metric, PCD-DAug consistently requires fewer statements to be inspected across all six fault localization methods compared to the other four data augmentation methods. PCD-DAug reduces the average number of statements to be examined to between 74.88% (for CNN-FL) and 99.23% (for Dstar) compared to PRAM, equating to reductions of 0.73% (100% – 99.23%) to 25.12% (100% – 74.88%).

PCD-DAug provides significant advantages in fault localization by achieving higher accuracy and reducing inspection effort compared to state-of-the-art data augmentation methods. This enhanced performance demonstrates PCD-DAug 's potential to streamline the fault localization process effectively.

Summary for RQ4: In RQ4, we analyzed the performance of PCD-DAug against three data augmentation methods. The results indicated that PCD-DAug performs better than Aeneas and Lamont, and slightly better than PRAM.

5 Discussion

5.1 Threats to Validity

The implementation of baselines and our approach. Our implementation of the baselines and PCD-DAug may potentially contain bugs. As shown in Table 7, PCD-DAug incorporates 3 residual blocks and 3 attention blocks. While this simplified design choice aims to balance complexity and efficiency, it may also reduce the model's capacity to capture more intricate patterns within the data. This could potentially result in underfitting, where the model fails to learn all relevant patterns, especially in cases where the data or the fault localization task requires a deeper model.

Table 7: Main Architecture and Parameter of PCD-DAug

Main Architecture and Parameter	Value
Number of convolution layers	13
Number of residual blocks	3
Number of GroupNorm layers	10
Number of attention blocks	3

Dataset-Specific Parameter Choices. For the two data augmentation methods, Aeneas and Lamont, both require a parameter that is strongly dependent on the dataset for dimensionality reduction, namely, the number of principal components (K). This parameter is inversely proportional to the number of statements in the dataset. In the experiments, K is automatically determined by comparing the number of executed statements across all faulty historical versions in the selected datasets. Therefore, differences in datasets may lead to variations in this parameter, potentially impacting experimental outcomes.

The generalizability. Our approach was tested on five representative programs, but its effectiveness on other programs may vary, as no dataset can encompass all fault scenarios. Further experiments on larger programs would be beneficial to confirm the approach's generalizability.

5.2 Reasons for PCD-DAug Is Effective

The reasons why PCD-DAug is more effective than the compared baselines are as follows: (1) PCD-DAug constructs a comprehensive fault semantic context and statistical context from program structure and statistical analysis perspectives. (2) The diffusion model, being a powerful generative approach, ensures effective sample generation without the concern of imbalances between generator and discriminator components, as seen in other models. (3) PCD-DAug generates failing test cases to balance the dataset, addressing the class imbalance issue.

6 Conclusion

In this paper, we propose PCD-DAug : a data augmentation approach using a Context-aware and PCA-enhanced diffusion model for fault localization. By employing dynamic program slicing, PCD-DAug constructs a fault semantic context that captures the dependencies between faulty statements. A revised PCA is then applied to capture the statistical context. Subsequently, a diffusion model is used to analyze the context matrix and generate synthetic failing test cases creating a class-balanced test suite, significantly enhancing the effectiveness of FL techniques. Our experimental results demonstrate that PCD-DAug is effective for FL.

In future work, We will explore the impact of data augmentation for FL in the latent space, rather than original space. Additionally, we will validate our approach's performance on more dataset.

References

[1] James A Jones. Fault localization using visualization of test information. In *Proceedings. 26th International Conference on Software Engineering*, pages 54–56. IEEE, 2004.

- [2] James A Jones and Mary Jean Harrold. Empirical evaluation of the tarantula automatic fault-localization technique. In *Proceedings of the 20th IEEE/ACM international Conference on Automated software engineering*, pages 273–282, 2005.
- [3] Xia Li, Wei Li, Yuqun Zhang, and Lingming Zhang. Deepfl: Integrating multiple fault diagnosis dimensions for deep fault localization. In *Proceedings of the 28th ACM SIGSOFT international symposium on software testing and analysis*, pages 169–180, 2019.
- [4] Yi Li, Shaohua Wang, and Tien Nguyen. Fault localization with code coverage representation learning. In *2021 IEEE/ACM 43rd International Conference on Software Engineering (ICSE)*, pages 661–673. IEEE, 2021.
- [5] Lee Naish, Hua Jie Lee, and Kotagiri Ramamohanarao. A model for spectra-based software diagnosis. *ACM Transactions on software engineering and methodology (TOSEM)*, 20(3):1–32, 2011.
- [6] Jeongju Sohn and Shin Yoo. Fluccs: Using code and change metrics to improve fault localization. In *Proceedings of the 26th ACM SIGSOFT International Symposium on Software Testing and Analysis*, pages 273–283, 2017.
- [7] Ming Wen, Junjie Chen, Yongqiang Tian, Rongxin Wu, Dan Hao, Shi Han, and Shing-Chi Cheung. Historical spectrum based fault localization. *IEEE Transactions on Software Engineering*, 47(11):2348–2368, 2019.
- [8] W Eric Wong, Vidroha Debroy, Yihao Li, and Ruizhi Gao. Software fault localization using dstar (d*). In *2012 IEEE Sixth International Conference on Software Security and Reliability*, pages 21–30. IEEE, 2012.
- [9] Zhuo Zhang, Yan Lei, Xiaoguang Mao, and Panpan Li. Cnn-fl: An effective approach for localizing faults using convolutional neural networks. In *2019 IEEE 26th International Conference on Software Analysis, Evolution and Reengineering (SANER)*, pages 445–455. IEEE, 2019.
- [10] Yan Lei, Tiantian Wen, Huan Xie, Lingfeng Fu, Chunyan Liu, Lei Xu, and Hongxia Sun. Mitigating the effect of class imbalance in fault localization using context-aware generative adversarial network. In *2023 IEEE/ACM 31st International Conference on Program Comprehension (ICPC)*, pages 304–315. IEEE, 2023.
- [11] Jian Hu and Yan Lei. A deep semantics-aware data augmentation method for fault localization. *Information and Software Technology*, 168:107409, 2024.
- [12] Jian Hu, Huan Xie, Yan Lei, and Ke Yu. A light-weight data augmentation method for fault localization. *Information and Software Technology*, 157:107148, 2023.
- [13] Huan Xie, Yan Lei, Meng Yan, Yue Yu, Xin Xia, and Xiaoguang Mao. A universal data augmentation approach for fault localization. In *Proceedings of the 44th International Conference on Software Engineering*, pages 48–60, 2022.
- [14] Rui Abreu, Peter Zoeteweij, and Arjan JC Van Gemund. On the accuracy of spectrum-based fault localization. In *Testing: Academic and industrial conference practice and research techniques-MUTATION (TAICPART-MUTATION 2007)*, pages 89–98. IEEE, 2007.
- [15] Zhuo Zhang, Yan Lei, Xiaoguang Mao, Meng Yan, Ling Xu, and Xiaohong Zhang. A study of effectiveness of deep learning in locating real faults. *Information and Software Technology*, 131:106486, 2021.
- [16] Wei Zheng, Desheng Hu, and Jing Wang. Fault localization analysis based on deep neural network. *Mathematical Problems in Engineering*, 2016(1):1820454, 2016.
- [17] Pavneet Singh Kochhar, Xin Xia, David Lo, and Shanping Li. Practitioners’ expectations on automated fault localization. In *Proceedings of the 25th international symposium on software testing and analysis*, pages 165–176, 2016.
- [18] Shin Hwei Tan, Jooyong Yi, Sergey Mechtaev, Abhik Roychoudhury, et al. Codeflaws: a programming competition benchmark for evaluating automated program repair tools. In *2017 IEEE/ACM 39th International Conference on Software Engineering Companion (ICSE-C)*, pages 180–182. IEEE, 2017.
- [19] Yanmin Sun, Andrew KC Wong, and Mohamed S Kamel. Classification of imbalanced data: A review. *International journal of pattern recognition and artificial intelligence*, 23(04):687–719, 2009.
- [20] Haibo He and Edwardo A Garcia. Learning from imbalanced data. *IEEE Transactions on knowledge and data engineering*, 21(9):1263–1284, 2009.
- [21] Cheng Gong, Zheng Zheng, Wei Li, and Peng Hao. Effects of class imbalance in test suites: an empirical study of spectrum-based fault localization. In *2012 IEEE 36th Annual Computer Software and Applications Conference Workshops*, pages 470–475. IEEE, 2012.
- [22] Mark Weiser. Program slicing. *IEEE Transactions on software engineering*, (4):352–357, 2009.
- [23] Petros Xanthopoulos, Panos M Pardalos, Theodore B Trafalis, Petros Xanthopoulos, Panos M Pardalos, and Theodore B Trafalis. Linear discriminant analysis. *Robust data mining*, pages 27–33, 2013.

- [24] Hervé Abdi and Lynne J Williams. Principal component analysis. *Wiley interdisciplinary reviews: computational statistics*, 2(4):433–459, 2010.
- [25] Hongyi Zhang, Moustapha Cisse, Yann N Dauphin, and David Lopez-Paz. mixup: Beyond empirical risk minimization. *arXiv preprint arXiv:1710.09412*, 2017.
- [26] Ian Goodfellow, Jean Pouget-Abadie, Mehdi Mirza, Bing Xu, David Warde-Farley, Sherjil Ozair, Aaron Courville, and Yoshua Bengio. Generative adversarial networks. *Communications of the ACM*, 63(11):139–144, 2020.
- [27] Jaehyeon Kim, Jungil Kong, and Juhee Son. Conditional variational autoencoder with adversarial learning for end-to-end text-to-speech. In *International Conference on Machine Learning*, pages 5530–5540. PMLR, 2021.
- [28] Divya Saxena and Jiannong Cao. Generative adversarial networks (gans) challenges, solutions, and future directions. *ACM Computing Surveys (CSUR)*, 54(3):1–42, 2021.
- [29] Hiralal Agrawal and Joseph R Horgan. Dynamic program slicing. *ACM SIGPlan Notices*, 25(6):246–256, 1990.
- [30] Fengxi Song, Zhongwei Guo, and Dayong Mei. Feature selection using principal component analysis. In *2010 international conference on system science, engineering design and manufacturing informatization*, volume 1, pages 27–30. IEEE, 2010.
- [31] Jonathan Ho and Tim Salimans. Classifier-free diffusion guidance. *arXiv preprint arXiv:2207.12598*, 2022.
- [32] Jonathan Ho, Ajay Jain, and Pieter Abbeel. Denoising diffusion probabilistic models. *Advances in neural information processing systems*, 33:6840–6851, 2020.
- [33] Diederik P Kingma, Max Welling, et al. Auto-encoding variational bayes, 2013.
- [34] Olaf Ronneberger, Philipp Fischer, and Thomas Brox. U-net: Convolutional networks for biomedical image segmentation. In *Medical image computing and computer-assisted intervention–MICCAI 2015: 18th international conference, Munich, Germany, October 5–9, 2015, proceedings, part III* 18, pages 234–241. Springer, 2015.
- [35] Ashish Vaswani, Noam Shazeer, Niki Parmar, Jakob Uszkoreit, Llion Jones, Aidan N Gomez, Łukasz Kaiser, and Illia Polosukhin. Attention is all you need. *Advances in neural information processing systems*, 30, 2017.
- [36] Yan Lei, Xiaoguang Mao, Ziying Dai, and Chengsong Wang. Effective statistical fault localization using program slices. In *2012 IEEE 36th Annual Computer Software and Applications Conference*, pages 1–10. IEEE, 2012.
- [37] Baowen Xu, Ju Qian, Xiaofang Zhang, Zhongqiang Wu, and Lin Chen. A brief survey of program slicing. *ACM SIGSOFT Software Engineering Notes*, 30(2):1–36, 2005.
- [38] Prafulla Dhariwal and Alexander Nichol. Diffusion models beat gans on image synthesis. *Advances in neural information processing systems*, 34:8780–8794, 2021.
- [39] Cheng Lu, Yuhao Zhou, Fan Bao, Jianfei Chen, Chongxuan Li, and Jun Zhu. Dpm-solver: A fast ode solver for diffusion probabilistic model sampling in around 10 steps. *Advances in Neural Information Processing Systems*, 35:5775–5787, 2022.
- [40] Xiaoyuan Xie, Tsong Yueh Chen, Fei-Ching Kuo, and Baowen Xu. A theoretical analysis of the risk evaluation formulas for spectrum-based fault localization. *ACM Transactions on software engineering and methodology (TOSEM)*, 22(4):1–40, 2013.
- [41] René Just, Darioush Jalali, and Michael D Ernst. Defects4j: A database of existing faults to enable controlled testing studies for java programs. In *Proceedings of the 2014 international symposium on software testing and analysis*, pages 437–440, 2014.
- [42] Spencer Pearson, José Campos, René Just, Gordon Fraser, Rui Abreu, Michael D Ernst, Deric Pang, and Benjamin Keller. Evaluating & improving fault localization techniques. *University of Washington Department of Computer Science and Engineering, Seattle, WA, USA, Tech. Rep. UW-CSE-16-08-03*, page 27, 2016.
- [43] Rui Abreu, Peter Zoeteweij, and Arjan JC Van Gemund. An evaluation of similarity coefficients for software fault localization. In *2006 12th Pacific Rim International Symposium on Dependable Computing (PRDC’06)*, pages 39–46. IEEE, 2006.
- [44] Rui Abreu, Peter Zoeteweij, and Arjan JC Van Gemund. Spectrum-based multiple fault localization. In *2009 IEEE/ACM International Conference on Automated Software Engineering*, pages 88–99. IEEE, 2009.
- [45] Haifeng Wang, Bin Du, Jie He, Yong Liu, and Xiang Chen. Ietc: An information entropy based test case reduction strategy for mutation-based fault localization. *IEEE Access*, 8:124297–124310, 2020.
- [46] Yichao Gao, Zhenyu Zhang, Long Zhang, Cheng Gong, and Zheng Zheng. A theoretical study: The impact of cloning failed test cases on the effectiveness of fault localization. In *2013 13th International Conference on Quality Software*, pages 288–291. IEEE, 2013.

- [47] Long Zhang, Lanfei Yan, Zhenyu Zhang, Jian Zhang, WK Chan, and Zheng Zheng. A theoretical analysis on cloning the failed test cases to improve spectrum-based fault localization. *Journal of Systems and Software*, 129:35–57, 2017.
- [48] Zhusuo Zhang, Yan Lei, Xiaoguang Mao, Meng Yan, Ling Xu, and Junhao Wen. Improving deep-learning-based fault localization with resampling. *Journal of Software: Evolution and Process*, 33(3):e2312, 2021.